In situ analysis of flocs

Rajat K. Chakraborti, Kevin H. Gardner, Jagjit Kaur and Joseph F. Atkinson

ABSTRACT

The physical properties of suspended particles and the relationship between particle size and structure were investigated. *In situ* properties of the aggregates in a coagulation–flocculation process were obtained using a non-intrusive image analysis technique. Derived properties, including density, porosity and the number of primary particles in a floc, were estimated from aggregate structure using a fractal approach, which better represents the distribution of mass in an aggregate, compared with a conventional Euclidean approach which considers uniform mass distribution in an assumed spherical shape. A spherical particle assumption overlooks the highly porous nature of real aggregates and underestimates volume, which subsequently influences coagulation and settling estimates in solid–liquid separation processes. The present results illustrate a strong inverse relationship between the fractal dimension and aggregate length, consistent with the idea that larger aggregates in general are more porous. In addition, correlations between the solids content, floc density and the number of primary particles that constitute a floc of a given size were established. It is suggested that the aggregation process produces flocs of constantly changing morphology and related physical properties. Overall, these findings can provide additional information for understanding and modeling suspended particle characteristics.

Key words | aggregate structure, density, floc properties, fractal geometry, number of particles, porosity

Rajat K. Chakraborti (corresponding author)
CH2M HILL, Inc.,
325 Hillcrest Drive,
Suite 125, Thousand Oaks CA 93063,
USA
Tel: +1 (805) 371 7822
Fax: +1 (805) 371 7818
E-mail: *rajat.chakraborti@ch2m.com*

Kevin H. Gardner
Environmental Research Group, Department of Civil Engineering,
University of New Hampshire,
336 Gregg Hall,
Durham NH 03824,
USA

Jagjit Kaur
CH2M HILL, Inc.,
1000 Willshire Blvd, 21st floor
Los Angeles CA 90017,
USA

Joseph F. Atkinson
Great Lakes Program, Department of Civil, Structural, and Environmental Engineering,
State University of New York at Buffalo,
207 Jarvis Hall, Buffalo NY 14260,
USA

NOTATION

l	characteristic length defined by the longest side of an aggregate
P	aggregate perimeter
A_s	projected area
V	aggregate volume
m_s	solid mass of aggregate
D_1	one-dimensional fractal dimension
D_2	two-dimensional fractal dimension
D_3	three-dimensional fractal dimension
ψ	a constant defined by $\psi = \zeta\xi/\xi_0$
ζ	packing factor
ξ_0	primary particle shape factor
ξ	aggregate shape factor
l_0	characteristic length for the primary particle
ρ_0	density of the primary particle
V_0	volume of primary particle
ρ_s	aggregate solid density
V_e	encased volume of the fractal aggregate
V_s	solid volume
ϕ	aggregate porosity
ρ	aggregate density
ρ_w	water density
rpm	revolution per minute
NTU	turbidity unit
s	half of the major axis of an ellipse
w	half of the minor axis of an ellipse
d_a	area equivalent diameter
m, n, p and q	empirical constants
C_1 and k	empirical constants
R	radius of the aggregate

doi: 10.2166/aqua.2007.063

R_0	radius of primary particle
N_0	number of primary particles
a and b	empirical constants

INTRODUCTION

Coagulation and flocculation of suspended particles and subsequent separation from the water column by settling and filtration are important steps in water treatment. These processes are also important for the fate and transport of natural suspended matter (Weilenmann *et al.* 1989; O'Melia & Tiller 1993; O'Melia 1998). Suspended particles are typically present as flocs, aggregates or clusters of particles in natural and engineered systems. The growth of aggregates, however, is a complicated process that depends on the physical, chemical and biological conditions of the system (Droppo *et al.* 1997; Han *et al.* 1997; Li & Logan 2001). Specifically, particle growth depends on the relative size of the colliding particles or clusters, their number density, surface charge and roughness, local shear forces and the suspending electrolyte (Tambo & Watanabe 1979; Gregory 1989; Amirtharajah & O'Melia 1990; Logan 1999). Characterization of floc properties based on real aggregate structure is essential to understand suspended particle behavior because the floc structure controls the effective drag acting on the floc (Li & Ganczarczyk 1987; Gregory 1989; Jiang & Logan 1991; Namer & Ganczarczyk 1993; Johnson *et al.* 1996; Droppo *et al.* 1997; Gregory 1998; Logan 1999; Li & Logan 2001). Recent studies (e.g. Droppo 2004; Sterling *et al.* 2004*a*,*b*; Atkinson *et al.* 2005) have demonstrated that vertical transport is altered because of changes in aggregate density, aggregate structure and floc stability. Non-intrusive, *in situ* measurements are of particular value for analyzing suspended particles, since the floc structure is not altered by the measurement process (Chakraborti 2004).

In conventional aggregation models, particles are assumed to be compact spheres, and under this assumption volume conservation can be easily computed in terms of changes in diameter, since when two particles collide and stick, the resulting volume is just the sum of the two original volumes and the diameter is found by assuming the resulting volume is again spherical. Other features of aggregation, including particle and hydrodynamic interactions, have also been explored on the basis of (assumed) spherical particles. In this approach the aggregate density, ρ, is essentially constant and equal to the density of the primary particles from which the aggregate was formed, since ρ is defined as the total mass of the aggregate divided by its volume. In addition, porosity, ϕ, is zero.

Mathematical modeling is used to simulate particle-bound contaminant transport and fate in developing sediment remediation strategies. These models depend on particle/floc size and shape, which changes with time and space (O'Connor 1988; O'Melia 1991; Droppo & Ongley 1992; O'Melia & Tiller 1993; Chapra 1997; Droppo *et al.* 1997). Although studies have reported that natural suspended particles are not spherical, a spherical and discrete particle approach with some assumed density is typically used in these analyses because it is difficult to assess the actual floc properties (Gibbs & Konwar 1982).

Recently, various measurement methods have been explored to find a suitable technique that does not disturb the fragile floc structure and preserves the natural process of floc formation (Kramer & Clark 1996; Allen 1997; Bushell *et al.* 2002). However, minor handling (e.g. transferring flocs using a pipette) and/or simplifying approximations have been a part of those analyses. For example, the Focused Beam Reflectance Method (FBRM) is based on the principle of laser light reflected by particles. However, FBRM requires theoretical and empirical data for converting from chord distribution to the conventional diameter distribution. Also, this method is susceptible to problems in the focal position of the laser light and it is sensitive to changes in the number, size and shape of particles.

In this study, a completely non-intrusive imaging method which avoids potential problems associated with sample collection and handling was used. Previously, Chakraborti *et al.* (2000, 2003) and Atkinson *et al.* (2005) documented the development of an imaging method for estimating fractal dimensions of suspended aggregates. The present work was targeted at understanding the application of this imaging technique on the evaluation of *in situ* physical properties of flocs based on real aggregate structure as represented by fractal geometry. These types of measurements can be used to answer questions involving floc physical properties that influence transport behavior in

suspension, and it is expected that results of this study will advance our capability to model aggregate interaction and transport.

THEORETICAL BACKGROUND

Recently, aggregates have been studied as fractal objects, where it is assumed that the relative arrangement of self-similar clusters within the aggregate structure is independent of the scale of observation (Li & Ganczarczyk 1987; Meakin 1988, 1999; Gregory 1989; Jiang & Logan 1991, 1996; Wiesner 1992; Johnson *et al.* 1996). In contrast, Euclidean geometry dictates that the volume and mass of a spherical particle increase with the cube of length (diameter) and surface area increases with the square of length. In fractal geometry, however, the exponent for either of these relationships can be a non-integral number. Various fractal dimensions are defined by (Jiang & Logan 1996)

$$P \propto l^{D_1};\ A_s \propto l^{D_2};\ V \propto l^{D_3} \tag{1}$$

where l is the characteristic length defined by the longest side of an aggregate, P, A and V are the aggregate perimeter, projected area and volume, respectively, and D_1, D_2 and D_3 are the one-, two- and three-dimensional fractal dimensions, respectively. Lower fractal dimension is associated with a more open (or 'stringy') structure (Meakin 1988, 1989, 1991, 1999; Jiang & Logan 1991). In essence, fractal geometry provides a means of expressing the mass distribution within an aggregate.

By taking into account the size and shape of primary particles and their packing architecture (i.e. mass distribution) in an aggregate, Logan and his co-workers (Jiang & Logan 1991, 1996; Johnson *et al.* 1996; Logan 1999) derived various aggregate properties in terms of fractal dimensions. The aggregate solid density (ρ_s) is expressed as

$$\rho_s = \frac{m_s}{V_e} = \rho_0 \psi^{D_3/3} \left(\frac{\xi_0}{\xi}\right) \left(\frac{l}{l_0}\right)^{D_3-3} \tag{2}$$

where $l =$ characteristic length defined by the longest side of an aggregate; $\psi =$ a constant defined by $\psi = \zeta\xi/\xi_0$; $\zeta =$ packing factor of aggregates; $\xi_0 =$ shape factor for the primary particles; $\xi =$ aggregate shape factor; $l_0 =$ characteristic length for the primary particles; $\rho_0 =$ density of the primary particles; $V_e =$ encased volume of the fractal aggregate; $m_{s=}$ solid mass of aggregate; $V_e =$ encased volume of the fractal aggregate; and $l_0 =$ characteristic length for the primary particles.

In addition, the porosity of the aggregate is expressed as

$$\phi = 1 - \psi^{D_3/3} \left(\frac{\xi_0}{\xi}\right) \left(\frac{l}{l_0}\right)^{D_3-3} \tag{3}$$

In this study, Equations (2) and (3) were used for baseline calculations of aggregate density and porosity, in order to develop simpler relationships among various floc properties that require minimal measurements or assumptions of floc characteristics.

MATERIALS AND METHODS

Materials

Water samples were collected from Lake LaSalle, a shallow lake located on the campus of the University at Buffalo, Buffalo, New York. The lake has an average depth of 3 m, with maximum depth of 8 m, and a total area of 243 000 m^2. The raw lake water contained moderate turbidity (22 NTU). A stock solution of alum was prepared by dissolving $Al_2(SO_4)_3.18\,H_2O$ (Fisher Scientific, Pittsburgh, PA) in deionized water to a concentration of 0.1M (0.2M as aluminum).

Experimental procedures

Standard jar tests were conducted for the samples coagulated with alum, which helped to produce large flocs (Chakraborti *et al.* 2000, 2003). After alum addition, the suspension was mixed rapidly ($\sim$ 100 rpm) for one minute and then slow-mixed (at about 25–35 rpm) for 20 min with a mean velocity gradient, $G = 20\,s^{-1}$. The mixing was then stopped and images of the aggregates in the jar were taken using a high resolution CCD camera. Images of aggregates were captured from various places in the jar. All the tests were conducted at a constant alum dose of 20 mg l^{-1}, with pH maintained at 6.5 by manual addition of acid (H_2SO_4) or base (NaOH) as required.

The experimental setup used for particle characterization is shown in Figure 1. Lighting was provided by a strobe lamp placed on the opposite side of the jar from the CCD camera, to provide a coherent back-lighting source. A public domain software package, NIH-Image (National Institute of Health, USA), was used to analyze the images. Before conducting the experiments, preliminary tests were conducted to ensure that the imaging procedures were providing accurate data and the pixel resolution was sufficient to provide accurate results for the range of particles analyzed (Chakraborti & Atkinson 2006). Monodisperse suspensions of several different latex particle sizes with known concentration were photographed to determine the accuracy of size analysis. The procedures used in this study were the same as used previously (Chakraborti *et al.* 2000, 2003).

The NIH-Image software fits an ellipse to each aggregate such that the area moments of inertia of the ellipse and the aggregate image are equal. This seems to be a valid approximation as most natural aggregates (see later) appear to be elongated and the mass distribution is non-uniform. This software measures the major and minor axes of the fitted ellipse, and the perimeter of each particle in an image. Details of the experiment, method and development of the image analysis technique are described elsewhere (Chakraborti *et al.* 2000, 2003; Atkinson *et al.* 2005).

RESULTS AND DISCUSSION

Images of flocs

Two close-up images of aggregates produced in the mixing jar are shown in Figure 2. It is apparent that these aggregates have a complex geometry, relatively high porosity and are non-spherical. The images show that the aggregate structure is an agglomerate of particles/clusters, with a highly irregular surface. The units of which the aggregates are composed (determined by labeling and identifying multiple size particles in the floc during image analysis) seem to be an agglomeration of several sub-flocs made up of primary particles. In addition, mass distribution is asymmetric about the centroid of the encasing ellipse. Qualitatively at least, this observation supports the characterization of natural aggregates in terms of an ellipsoidal shape and fractal geometry. It is logical to assume these aggregates should experience different collision rates than are conventionally assumed using Euclidean geometry, which considers uniform mass distribution in the assumed spherical shape of the aggregates.

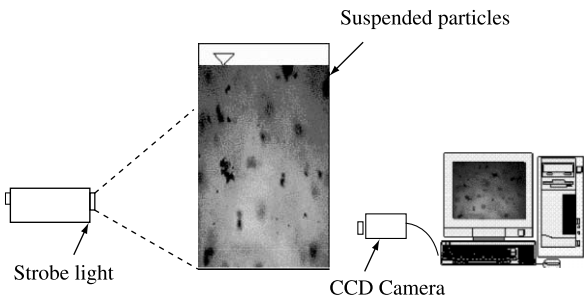

Figure 1 | Experimental setup for *in situ* particle characterization studies.

Statistical analyses of aggregates

Statistical data for aggregate size are presented in Table 1 for 58 aggregates. The average length of the major axis of these aggregates was 118 μm ± 81 μm (standard deviation), while aggregate sizes (of major axis of aggregates) ranged between 333 μm and 18 μm. Similarly, the minor axis of the aggregates ranged widely, from 7 to 195 μm, with an average value of 74 μm ± 51 μm. The average length of the major axis is more than one and half times larger than that of the minor axis, which demonstrates the general elongation in particle shape.

A wide variation in both perimeter and area can be seen, as indicated by the relatively large standard deviations for these parameters in Table 1. Based on the fitted ellipses, the perimeter can be estimated by

$$P = 2\pi\sqrt{\frac{1}{2}(s^2 + w^2)} \tag{4}$$

where s is half of the major axis and w is half of the minor axis of the fitted ellipse. It is interesting to note that the measured average perimeter (547 μm) is much larger than the calculated perimeter (Equation (4)) of the fitted ellipse (309.41 μm) when the averages of the major and minor axes were used (Table 1).

These measurements are consistent with the observation of non-sphericity of the aggregates. The perimeter

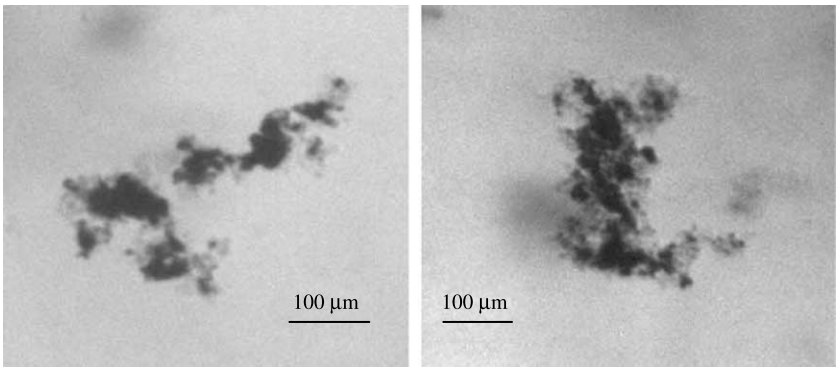

Figure 2 | *In situ* images of large, porous, loosely bound, highly branched, and irregular aggregates.

(and corresponding surface area) of the aggregate is important for processes such as flocculation and adsorption. Thus, accurate measurement of this parameter should be important in the development and testing of better simulation models, especially since the fitted perimeter from Euclidean geometry (based on the spherical shape assumption) is most often used for designing various processes for engineered and natural aquatic systems. For example, the measured average perimeter (547 μm) of the aggregates was found to be significantly greater than the calculated (fitted) perimeter, πd_a (411 μm), when the area equivalent diameter (d_a) was calculated from the measured projected area of the aggregates. This deviation in perimeter estimates was due to non-sphericity in aggregate shape.

Aggregate size distribution

Figure 3 shows the aggregate size distribution plot, where the major axis of the aggregates (l) is taken as the measurement of aggregate size and the number of aggregates present in the aggregate bin size is the corresponding y-axis value. The flocculated particles represent a wide range of sizes with peaks in the size distribution at about 90 μm and 200 μm. The presence of various sizes of aggregates suggests that there are many possibilities for aggregate collisions to take place (Lawler 1997). The heterogeneity in aggregate size and shape is expected to lead to variable rates for processes such as aggregation and disaggregation under various physical, chemical and hydrodynamic conditions.

Table 1 | Summary of statistical analysis of aggregates using imaging technique

Parameters	Mean	Std. dev.	Median	Maximum	Minimum
Perimeter (μm)	547	463	682	1823	68
Projected area (μm^2)	9600	10 846	12 296	51 190	195
Major axis (μm)	118	81	108	333	18
Minor axis (μm)	74	51	97	195	7

Roundness factor

Figure 4 shows calculations of the distribution of roundness factors for the aggregates, where the roundness factor is defined as $4\pi A_s/P^2$, where P is the perimeter of flocs. These calculations are particularly sensitive to the 'roughness' of the boundaries, through the values for P. Most of the particles had roundness factors of 0.6 or below (some as low as 0.2), indicating irregularity and elongation of shape

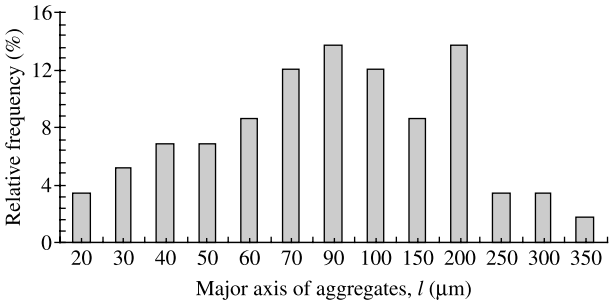

Figure 3 | Particle size distribution of flocs.

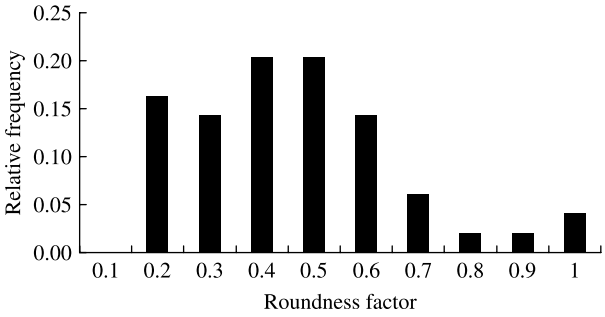

Figure 4 | Distribution of roundness factors of flocs.

(a circle has a roundness factor of 1). The median value for this distribution was 0.45; the aggregates in this study showed a pronounced effect of irregularities and non-circularity in shape.

The above results show that the aggregates were highly elongated and presumably affected differently by hydrodynamic effects than spherical particles would have been. Such variability in the natural floc size and irregularity in shape are important characteristics in evaluating effectiveness in separation processes since they influence various properties of suspended particles including the settling characteristics. In addition, fluid drag should be different for these irregularly shaped aggregates, in comparison to particles analyzed as spheres (Johnson *et al.* 1996; Logan 1999). This is an important observation because it has been found that the volume of a sphere is always greater than the volume of the corresponding ellipse. Thus, using the equivalent sphere approach will overestimate the aggregate volume, which subsequently influences coagulation and settling estimates in solid–liquid separation processes. Drag force based on aggregate shape is an important property to understand floc behavior in suspension. In addition, surface roughness and non-circularity in particle shape are important factors for evaluating collision rates, settling rates and aggregation kinetics (Atkinson *et al.* 2005).

Fractal analysis

Various fractal dimensions were calculated according to Equation (1) (from the slope of the log–log plot of characteristic size vs. perimeter, projected area, or volume of aggregates) and yielded the following values: $D_1 = 1.09 \pm 0.09$ ($r^2 = 0.92$), $D_2 = 1.65 \pm 0.10$ ($r^2 = 0.93$) and $D_3 = 2.12 \pm 0.50$ ($r^2 = 0.70$). The approach used here to calculate the fractal dimensions does not measure the fractal dimension for a single particle. Instead, it resolves observed properties (size and mass) for an ensemble of particles. This provides an averaged value for the whole population of particles and aggregates in a particular sample.

For D_1, a value somewhat greater than 1 is expected since the perimeter of the irregular fractal objects increases with particle size at a different rate (generally higher) than for a spherical object (also shown earlier with the statistical analyses of flocs). With D_2 significantly less than 2 (at least according to the fractal geometry concepts), it is concluded that aggregates have a more 'open' structure and are less dense than an equivalent sphere of the same mass (see Figure 2). In order to calculate D_3 an ellipsoidal shape was used with the thickness in the direction normal to the viewing direction assumed to be the same as the short axis of the ellipse fitted to the two-dimensional images. Volume was then calculated by rotating the fitted ellipse about the major axis (Chakraborti *et al.* 2000). A D_3 value greater than 2 suggests that aggregation was a reaction-limited aggregation (RLA) process, where aggregation is limited by electrostatic forces on the interacting particle/cluster surfaces. In RLA, a small fraction of collisions successfully result in attachment, unlike the traditional diffusion-limited aggregation (DLA) approach in which all collisions are successful. In general, if aggregation is amenable upon particle contact (as in a DLA approach), a lower fractal dimension results, while in reaction-limited systems a greater number of collisions is necessary before attachment, resulting in greater penetration of particles into aggregates. This results in higher fractal dimensions, characteristic of a more densely packed aggregate.

Floc density and porosity

Figure 5 shows aggregate porosity and density as a function of aggregate size, taken as the major axis of the ellipse fitted to each aggregate. Similar relationships between floc size, density and porosity have been observed in several previous studies (Tambo & Watanabe 1979; Klimpel *et al.* 1986; Amos & Droppo 1996; Droppo *et al.* 1997). These properties are important for settling and general transport calculations

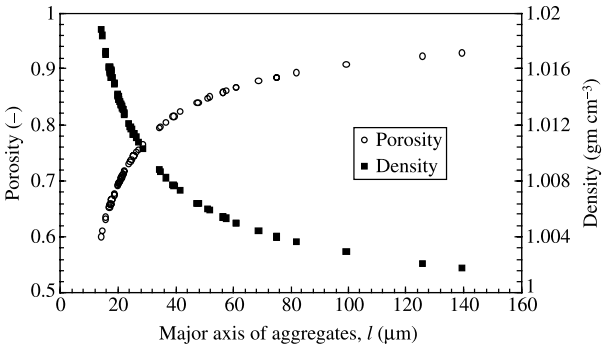

Figure 5 | Aggregate properties as a function of size for measured data for density and porosity.

(Gregory 1997). Equation (2) was used to calculate floc density and Equation (3) was used for floc porosity. With the help of the imaging technique, various parameters in Equations (2) and (3) were evaluated from fractal dimension and the floc properties and the packing factors were assigned from the shape of the aggregates. The shape factor (ξ) of the aggregates was calculated as (Jiang & Logan 1991)

$$\xi = \frac{A_s}{l_0^{(2-D_2)} l^{D_2}} \tag{5}$$

where $A_s =$ projected area of aggregates.

The magnitude of the packing factor depends on the arrangement of primary particles relative to one another and describes the state of mass distribution. For example, for a simple cubic packing (or lattice) of uniform spheres and a rhombohedral packing, the packing factors are 0.53, and 0.74, respectively (Vicsek 1992; Logan 1999). Feder (1988) estimated the packing factor of ellipsoidal aggregates as

$$\zeta = \frac{\pi s}{3w\sqrt{2}} \tag{6}$$

In this study, Equation (6) was used to estimate the packing factor of aggregates based on the major and minor axes of the fitted ellipses.

In this calculation, the density of the primary particles forming the floc was assumed to be 2.65 g cm^{-3}, corresponding to clay or silt particles. For larger aggregates, the major portion of the aggregate contains pores and porosity varied between 0.92 and 0.99. Floc density varied from 1.01 to 1.10 g cm^{-3}, considerably less than the primary particle density. It is observed from Figure 5 that, due to the large porosity (also see Figure 2), the flocs approached a density close to that of water.

In order to represent density and porosity in a more convenient way, with a simple relationship requiring minimal measurements for floc parameters, power law relationships were sought of the form

$$\rho = ml^{-n} \tag{7}$$

$$\phi = pl^{q} \tag{8}$$

where m, n, p and q are empirical constants determined by regression of data and depend on experimental conditions. In the present study, coefficients corresponding to best fit of the computed curves were: $m = 1.23$, $n = 0.03$, $p = 0.87$ and $q = 0.02$ (Figure 5). Both the density and porosity relationships have a high correlation. The floc density estimates from the present study also agree well with the observations by Glasgow & Hsu (1984), who reported correlation of the aggregate density with the pH of the solution and determined density from permeability measurements for kaolin–polymer aggregates. At pH 10.82, their correlation yielded: $m = 1.05$ and $n = 0.03$, with $r^2 = 0.89$.

Combining the above relationships between floc density and porosity and eliminating characteristic length from Equations (7) and (8), the aggregate density can be described in terms of porosity as

$$\rho = C_1 \phi^{-k} \tag{9}$$

where C_1 and k are empirical constants given by

$$C_1 = mp^k \tag{10}$$

$$k = \frac{n}{q}. \tag{11}$$

After substituting the values determined in the present study in Equations (10) and (11), it was found that $C_1 = 1.06$ and $k = 1.50$. Although these coefficients are system-dependent, these values would help provide estimates for density or porosity.

It is important to mention that the particular shear regime and floc development conditions applied in this study are an important factor in comparing the present

results with other literature values discussed above. It is to be noted that the first minute of fast stirring is probably the most important time for governing the floc structure. The subsequent slow mixing would have served to increase the size of the flocs by allowing aggregation between flocs formed in the initial period (Gregory & Chung 1995; Liem *et al.* 1999). However, further research is necessary to estimate the ranges of constants and exponents from various experimental conditions and for different aggregates from various origins, including flocs formed in the presence of natural organic matter.

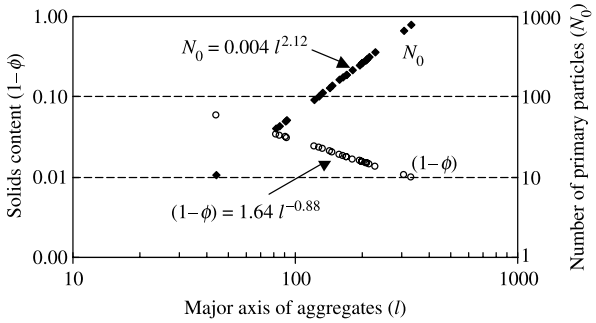

Figure 6 | Solids content and number of primary particles contained in the aggregates. For solids content $(1 - \phi)$: median = 0.02, range = 0.01–0.06; for N_0: median = 408, range = 23–1700.

Aggregate morphology, mass distribution and aggregate physical properties

It has been seen from the images of aggregates (Figure 2) that the coagulation–flocculation process leads to development of heterogeneous structure (with elongated shape) due to the non-homogeneous distribution of the primary particles or mass. The number of primary particles in an aggregate is an indication of porosity and size of a floc. A non-uniform distribution of primary particles within an aggregate structure makes it difficult to predict the behavior of suspended particles. With the spreading out of primary particles (of constant mass), the density of an aggregate decreases for any given size and the distribution of mass affects floc stability and floc properties in suspension.

The relationship correlating the number of primary particles in the aggregate with the size of the aggregate and fractal dimension is given by (Gardner 1999)

$$N_0 = \zeta\left(\frac{R}{R_0}\right)^{D_3} \tag{12}$$

where R is the radius of the aggregate, R_0 is the radius of primary particles that constitute the structure of the aggregate, ζ is the packing factor and N_0 is the number of primary particles in the aggregate. The ratio R/R_0 represents a dimensionless aggregate size.

Figure 6 shows a plot of the number of primary particles (estimated from Equation (12) using the major axis of aggregates and 10 μm diameter primary particles) and the solids content (represented as $(1 - \phi)$) as a function of the long axis of aggregates. It should be noted that the number of primary particles increases with an increase in aggregate size and mass. Since the aggregates analyzed in this study were highly porous, the solids content was typically low. Conversely, a denser object is characterized with a higher number of primary particles (for a given size). The number of primary particles ranged between 23 and 1700, with a median value of 408, whereas $(1 - \phi)$ varied between 0.01 and 0.06. The floc size varied between 40 and 333 μm. As shown in Figure 6, relatively smaller aggregates have a higher solids content, but fewer primary particles. The effect of size is more pronounced on the estimation of primary particles than on the solids content (see exponents in the equations for best fit).

The relationship between solids content and the number of primary particles can also be evaluated by the following regression:

$$(1 - \phi) = aN_0^{-b} \tag{13}$$

where a and b are empirical constants determined by regression of data over the range of sizes observed. In the present study, $a = 0.43$ and $b = 0.41$ were obtained. The result shown in Figure 6 is in agreement with the measurements by Klimpel *et al.* (1986) for floc size and floc solid fraction relationship within the size range used in this study. However, they studied a wider range of sizes for aggregating quartz (~10 μm) particles coagulated with non-ionic polymer. When the solids content is plotted against the particle size from their data, it can be fitted with $(1 - \phi) = 12.60d^{-0.88}$ ($r^2 = 0.97$), where d is the aggregate diameter. This expression is very close to the relation found in this study and, interestingly, the exponent is the same

(see Figure 6). This result suggests that these studies may have had the same shearing regime (Liem *et al.* 1999).

Physically, porosity measures voids in an aggregate and it is also a measure of density, resulting from various aggregation processes. Thus, it is of interest to establish a relationship between the number of primary particles and the density. The net gravitational force for settling depends on the difference between ρ and ρ_w, which can be written as

$$\rho - \rho_w = (1 - \phi)(\rho_0 - \rho_w). \tag{14}$$

From Equations (13) and (14) and substituting for values determined in this study (with fewer primary particles), it can be shown that N_0 is related to the floc density as

$$N_0 = \left[\frac{1}{a}\left(\frac{\rho_a - \rho_w}{\rho_0 - \rho_w}\right)\right]^{1/b}. \tag{15}$$

The numbers are high with higher values of a and lower values of b, which represents aggregates with larger solids content (see Equation (13)). Since the density of primary particles is higher than the density of an aggregate, the denominator in the parentheses of Equation (15) is always greater than the numerator, which will result in a ratio less than 1. Depending on the number of primary particles within a floc, the density will vary. In addition to the numbers, the arrangement or packing of primary particles is important in determining the fate of suspended material.

In order to understand floc behavior in suspension, it is important to understand aggregate settling rates based on aggregate structure or fractal dimension. Settling properties of suspensions are a function of gravity, buoyancy and drag forces. Drag on an aggregate moving through the water column depends on the flow of water around and possibly through the aggregate, which in turn depends on overall shape, porosity and distribution of primary particles within the aggregate structure. For example, flow through an aggregate's pore structure will likely result in significantly different drag forces than flow around a sphere or ellipse. This, however, is a current subject of research and measurement of a number of particles in a floc, aggregate shape and fractal dimension, as done in this work, does not lead directly to a complete understanding of floc behavior.

Johnson *et al.* (1996) discussed the impact of variable pore structure and size on the drag coefficient or the hydrodynamic friction estimates with reference to fractal (natural aggregates). They reported that large pores resulting in passage of water through its structure (predominantly with non-spherical shape) produce a smaller overall drag per total cross sectional area for the fractal aggregate than calculated for an impermeable or permeable spherical aggregate. Li & Logan (2001) described the larger holes formed by the principal clusters regulate flow of water and, therefore, the drag. They described that the most important factor in the hydraulic properties of the aggregate is the number of clusters the primary particles separated into, as the number and size of these clusters determines the pore size and overall permeability of the aggregate. As shown in Figure 2, clusters (particularly the left image) of various size and shape would experience variable drag in the floc structure.

CONCLUSIONS

In this study a simple relationship between floc density and porosity was established in characterizing aggregates based on minimal *in situ* measurements. It was found that ϕ is related to size, and indirectly to D_2 and D_3. This study also evaluated the number of primary particles in an aggregate, which is directly related to floc mass. The images illustrated the non-uniform distribution of mass and irregular shape of the aggregates. Large aggregates with low fractal dimensions have lower density with less solids content, higher porosity and larger number of primary particles when compared with relatively compact aggregates with higher fractal dimension. The analysis presented here (assuming an encased volume concept for aggregates along with the distribution of primary particles inside the aggregate structure) integrates the fact that the volume of an aggregate is larger than the sum of the volumes of the primary particles from which they are formed. Large aggregates contain water and this in turn leads to a lower density than that of compact spherical flocs composed of parent material. Quite appropriately, it has been shown and quantified that the density of a floc is not a constant property of a growing aggregate, rather it generally decreases with increasing size. Basic properties such as density and porosity of aggregates were shown to be

functions of size, which was derived from fractal geometry concepts, and that information can be easily incorporated in dynamic (time and space varying) estimations of particle properties. Along with relatively high porosity, these results show that the solid sphere assumption has obvious drawbacks, although it clearly has facilitated progress in aggregation theory.

This study has benefited greatly from the application of an imaging technique which enabled us to better understand the significance of floc properties explained by fractal geometry, as an indicator of aggregation kinetics derived from real floc characteristics. Chakraborti *et al.* (2003) have shown that the compactness of floc changes with time, resulting in changes in fractal dimension. Accordingly, temporal variability in floc properties appears to be a significant phenomenon, requiring further study both from a theoretical and experimental point of view.

ACKNOWLEDGEMENTS

The authors would like to thank Dr. John E. VanBenschoten of the Department of Civil, Structural and Environmental Engineering of the University at Buffalo and Dr. J.V. DePinto from Limno-Tech, Inc., for valuable comments and suggestions. The New York Sea Grant Institute is also gratefully acknowledged for partial support of the project under Grant R/CTP-21.

REFERENCES

Allen, T. 1997 *Particle Size Measurement*, vol. I. Chapman & Hall, London.

Amirtharajah, A. & O'Melia, C. R. 1990 Coagulation processes: destabilization, mixing, and flocculation. In *AWWA Water Quality & Treatment*. McGraw-Hill, New York, pp. 269–365.

Amos, C. L. & Droppo, I. G. 1996 *The Stability of Remediated Lake Bed Sediment*. Hamilton Harbor, Lake Ontario, Canada, Geological Survey of Canada open file report no. 2276.

Atkinson, J. F., Chakraborti, R. K. & VanBenschoten, J. E. 2005 Effects of floc size and shape in particle aggregation. In Droppo, I. G., Leppard, G. G., Liss, S. N. & Milligan, T. G. (eds) *Flocculation in Natural and Engineered Environmental Systems*. CRC Press, Boca Raton, FL, chapter 5.

Bushell, G. C., Yan, Y. D., Woodfield, D., Raper, J. & Amal, R. 2002 On techniques for the measurement of the mass fractal dimension of aggregates. *Adv. Colloid Interface Sci.* **95**, 1–50.

Chakraborti, R. K. 2004 *Application of Fractal Concepts for Analysis and Modeling of Particle Aggregation*. PhD Dissertation, Department of Civil, Structural, and Environmental Engineering, University at Buffalo, Buffalo, NY.

Chakraborti, R. K. & Atkinson, J. F. 2006 Dependence of perceived aggregate size on pixel resolution using an imaging method. *J. Wat. Suppl: Res. Technol. – AQUA* **55**(7–8), 439–451.

Chakraborti, R. K., Atkinson, J. F. & VanBenschoten, J. E. 2000 Characterization of alum floc by image analysis. *Environ. Sci. Technol.* **34**(18), 3969–3976.

Chakraborti, R. K., Gardner, K. H., Atkinson, J. F. & VanBenschoten, J. E. 2003 Changes in fractal dimension during aggregation. *Wat. Res.* **37**(4), 873–883.

Chapra, S. C. 1997 *Surface Water Quality Modeling*. McGraw Hill, New York.

Droppo, I. G. 2004 Structural controls on floc strength and transport. *Can. J. Civil Engr.* **31**, 569–578.

Droppo, I. G., Leppard, G. G., Flannigan, D. T. & Liss, S. N. 1997 The freshwater floc: a functional relationship of water and organic and inorganic floc constituents affecting suspended sediment properties. *Wat. Air Soil Pollut.* **99**, 43–54.

Droppo, I. G. & Ongley, E. D. 1992 The state of suspended sediment in the freshwater fluvial environment: a method of analysis. *Wat. Res.* **26**(1), 65–72.

Feder, J. 1988 *Fractals*. Plenum Press, New York.

Gardner, K. H. 1999 Kinetic models of colloid aggregation. In Hsu, J. P. (ed.) *Interfacial Forces and Fields: Theory and Applications*. Marcel Dekker, New York, pp. 509–550.

Gibbs, R. J. & Konwar, L. 1982 Effect of pipetting on mineral flocs. *Environ. Sci. Technol.* **16**, 119–121.

Glasgow, L. A. & Hsu, J. P. 1984 Floc characteristics in water and wastewater treatment. *Particle Sci. Technol.* **2**, 285–303.

Gregory, J. 1989 Fundamentals of flocculation. *CRC Crit. Rev. Environ. Con.* **19**(3), 185–230.

Gregory, J. 1997 The density of particle aggregates. *Wat. Sci. Technol.* **36**(4), 1–13.

Gregory, J. 1998 The role of floc density in solid-liquid separation. *Filt. Sep.* **35**(4), 367–371.

Gregory, J. & Chung, H. 1995 Continuous monitoring of floc properties in stirred suspensions. *J. Wat. Suppl: Res. Technol. – AQUA* **44**(3), 125–131.

Han, M., Lee, H., Lawler, D. F. & Choi, S. 1997 Collision efficiency factor in brownian coagulation (αBr) including hydrodynamics and interparticle forces. *Wat. Sci. Technol.* **36**(4), 69–75.

Jiang, Q. & Logan, B. E. 1991 Fractal dimensions of aggregates determined from steady state size distributions. *Environ. Sci. Technol.* **25**(12), 2031–2038.

Jiang, Q. & Logan, B. E. 1996 Fractal dimensions of aggregates from shear devices. *J. AWWA* **88**(2), 100–113.

Johnson, C. P., Li, X. & Logan, B. E. 1996 Settling velocities of fractal aggregates. *Environ. Sci. Technol.* **30**, 1911–1918.

Klimpel, R. C., Dirican, C. & Hogg, R. 1986 Measurement of agglomerate density in flocculated fine particle suspensions. *Part. Sci. Technol.* **4**, 45–59.

Kramer, T. A. & Clark, M. M. 1996 The measurement of particles suspended in a stirred vessel using microphotography and digital image analysis. *Part. Part. Syst. Charact.* **13**, 3–9.

Lawler, D. F. 1997 Particle size distributions in treatment processes: theory and practice. *Water Sci. Technol.* **36**(4), 15–23.

Li, D. & Ganczarczyk, J. J. 1987 Stroboscopic determination of settling velocity, size and porosity of activated sludge flocs. *Wat. Res.* **21**, 257–262.

Li, X. & Logan, B. E. 2001 Permeability of fractal aggregates. *Wat. Res.* **35**(14), 3373–3380.

Liem, L. E., Smith, D. W. & Stanley, S. J. 1999 Turbulent velocity in flocculation by means of grids. *J. Environ. Engng. ASCE* **3**, 224–233.

Logan, B. E. 1999 *Environmental Transport Processes*. John Wiley & Sons, New York.

Meakin, P. 1988 Fractal aggregates. *Adv. Colloid Interface Sci.* **28**, 249–331.

Meakin, P. 1989 Simulations of aggregation processes. In Avnir, D. (ed.) *The Fractal Approach to Heterogeneous Chemistry*. John Wiley & Sons, New York, pp. 131–158.

Meakin, P. 1991 Fractal aggregates in geophysics. *Rev. Geophys.* **29**, 317–354.

Meakin, P. 1999 A historical introduction to computer models for fractal aggregates. *J. Sol-Gel Sci. Technol.* **15**, 97–117.

Namer, J. & Ganczarczyk, J. J. 1993 Settling properties of digested sludge particle aggregates. *Wat. Res.* **27**, 1285–1294.

O'Connor, D. J. 1988 Models of sorptive toxic substances in freshwater systems. III Streams and rivers. *J. Environ. Engng. ASCE* **114**(3), 552–574.

O'Melia, C. R. 1991 Practice, theory, and solid-liquid separation. *J. Wat. Suppl.: Res. Technol. – AQUA* **40**(6), 371–379.

O'Melia, C. R. 1998 Coagulation and sedimentation in lakes, reservoirs and water treatment plants. *Wat. Sci. Technol.* **37**(2), 129–135.

O'Melia, C. R. & Tiller, C. L. 1993 Physicochemical aggregation and deposition in aquatic environments. In Buffle, J. & van Leewen, H. P. (eds) *Environmental Particles*, vol. 2. Lewis Publishers, Boca Raton, FL, pp. 353–386.

Sterling, M. C., Bonner, J. S., Ernest, A. N. S., Page, C. A. & Autenrieth, R. A. 2004*a* Characterizing aquatic sediment-oil aggregates using in situ instruments. *Mar. Pollut. Bull.* **48**, 533–542.

Sterling, M. C., Bonner, J. S., Page, C. A., Fuller, C. B., Ernest, A. N. S. & Autenrieth, R. A. 2004*b* Modeling crude oil droplet-sediment aggregation in nearshore waters. *Environ. Sci. Technol.* **38**(17), 627–634.

Tambo, N. & Watanabe, Y. 1979 Physical characteristic of flocs: I. The floc density function and aluminum floc. *Wat. Res.* **13**, 409–419.

Vicsek, T. 1992 *Fractal Growth Phenomena*. World Scientific, Singapore.

Weilenmann, U., O'Melia, C. R. & Stumm, W. 1989 Particle transport in lakes: models and measurement. *Limnol. Oceanogr.* **34**(1), 1–18.

Wiesner, M. R. 1992 Kinetics of aggregate formation in rapid mix. *Wat. Res.* **26**(3), 379–387.

First received 15 March 2006; accepted in revised form 2 August 2006